



# GALVANIC CORROSION-RESISTANT CARBON FIBER METAL LAMINATES

Wen-Xue Wang, Yoshihiro Takao, Terutake Matsubara  
RIAM, Kyushu University, 6-1 Kasuga-koen Kasuga-shi Fukuoka, 816-8580, Japan

**Keywords:** *Fiber Metal Laminates, Carbon Fiber Aluminum laminate, Galvanic Corrosion, Nano-composite Coating, Sulfuric Anodizing, Hybrid Sol-Gel Coating*

## Abstract

*In this paper, a galvanic corrosion-resistant carbon fiber metal laminate (CARALL) is developed. Aluminum alloy 2024-T3 is selected as the metal layer. A surface treatment technique combining a sulfuric acid anodizing with a hybrid sol-gel coating for the aluminum alloy is developed to prevent CARALL from galvanic corroding. Electrochemistry tests are conducted to evaluate the properties of electrochemistry of aluminum alloy treated by the present method. The test results prove that the combination of sulfuric acid anodizing and hybrid sol-gel coating can provide good protection against the galvanic corrosion in CARALL. Moreover, aluminum alloy sheets and carbon fiber/epoxy prepreg are stacked and cured in an autoclave to fabricate CARALL. The cross-section of fabricated CARALL is investigated by scanning electron microscope (SEM) and electron probe micro analyzer (EPMA). Well bonded thin interlayer consisting of composite layers is formed between aluminum alloy and carbon fiber-reinforced epoxy layer. Corrosion tests of CARALL and aluminum alloy are conducted, the present CARALL shown excellent corrosion resistance. Three-point and five-point bend tests are conducted to evaluate the interlaminar shear strength of the CARALL.*

## 1 Introduction

Fiber reinforced composites have been widely used in the many industries such as aircraft, aerospace, automobiles, ships and civil constructions. In the recent years, among the families of fiber reinforced composites, a relatively new family named as fiber metal laminates (FMLs) or fiber-reinforced metal laminates (FRMLs) have attracted considerable attentions [1-3]. FMLs are a kind of

hybrid composite materials consisting of metal sheets bonded to fiber reinforced plastic (FRP) layers. This kind of hybrid composite materials has been studied at Delft University of Technology since the late 1970's. Aramid fiber reinforced plastics/aluminum alloy (AFRP/Al), called as ARALL, and glass fiber reinforced plastic/aluminum alloy (GFRP/Al), called as GLARE, have been successfully developed at Delft University of Technology and the GLARE has been used in A380 as a new structural material.

In the early stage of the study of FMLs, the carbon fiber reinforced plastic (CFRP) was also considered as a potential composite layers combined with aluminum alloy to fabricate carbon fiber reinforced aluminum laminate (CFRP/Al-FRML) since the CFRP has many advantages than AFRP and GFRP, such as higher specific stiffness and strength. For the sake of simplicity and according to a previous paper [4], CFRP/Al-FRML will be renamed as CARALL in the following text of this paper. Many researchers have made a lot of efforts to develop CARALL over the last decades. In particular, the researchers at Delft University of Technology and at University of Sydney have made great contribution to the fabrication technology and the characterization of CARALL. However, up-to-date two major problems to the development of CARALL are still unsolved yet. The first is the galvanic corrosion problem between carbon and aluminum alloy due to the difference of natural potential between carbon and aluminum alloy. The galvanic corrosion may seriously reduce the strength of aluminum during the serving period if a valid protection is not provided for aluminum alloy. The second is the large thermal residual stresses problem in aluminum alloy due to large mismatch of the coefficient of thermal expansion between CFRP and aluminum alloy. Large thermal residual stresses

induce low static strength and low fatigue strength of CARALL. Therefore, how to solve these two problems becomes a key point in the development of practicable CARALL.

Vermeeren gave a detail description on the researches of CARALL conducted at Delft University of Technology in a report [5]. In order to overcome the galvanic corrosion problem, a thermoplastic interlayer (PolyEtherImide, PEI) of approximate 0.02 mm thickness or a GFRP layer of about 0.1 mm thickness was inserted between CFRP layer and aluminum alloy sheet to isolate the aluminum alloy from CFRP. Test results showed that this method could give good protection for CARALL from the galvanic corrosion. However, the mechanical experimental results revealed that the interlayer caused the reduction of stiffness and the fatigue strength of CARALL. Therefore practically effective CARALL have not been commercialized up-to-date. Similarly, Lin and his co-researchers also utilized a GFRP layer to isolate the aluminum alloy from CFRP [6]. Fatigue strength and thermal residual stresses were investigated. A post-cure stretching method was used to eliminate the residual stress in the aluminum alloy of unidirectional CARALL. Parallel to these studies, Mai and his co-researchers at University of Sydney have conducted many studies on the characterization of mechanical and adhesion properties of CARALL [7-12]. The research results showed that CARALL has many advanced mechanical properties than ARALL and GLARE if the galvanic corrosion problem is solved. However, no studies on the galvanic corrosion problem can be found from their open reports and published papers. Hence, a valid technology that can not only provide a protection for aluminum alloy from galvanic corrosion but also does not reduce the stiffness and strength of CARALL is necessary for the development of practically effective CARALL.

In addition to the researches on the galvanic corrosion of CARALL, the corrosion protection of aluminum alloy is also a general problem. In most cases of aircraft and aerospace industries, chromic acid anodizing surface treatment is employed for the corrosion protection of aluminum alloy because the chromate conversion coating is extremely effective and widely used as corrosion inhibitors for high strength aluminum alloys. On the other hand, unfortunately, the hexavalent chromium is environmentally hazardous. The use of chromates and other chromium containing compounds has been limited since 1982 due to their carcinogenic effects. Recently, much interesting has been focused on

developing new chromate-free surface treatment technology for aluminum alloy [13]. An attractive coating technology is the inorganic/organic hybrid sol-gel coating [14-16]. Referring to this trend, therefore we recognize that the environmental effects have to be considered in the research to solve the galvanic corrosion problem of CARALL.

In this paper, the main attention is focused on the galvanic corrosion problem of CARALL. A galvanic corrosion-resistant CARALL is developed based on a new surface treatment method, namely nano-composite coating. Aluminum alloy 2024-T3 is selected as the metal layer. Nano-composite coating surface treatment method consists of a sulfuric acid anodizing process and a  $S_iO_2$  nano-particle reinforced inorganic/organic hybrid sol-gel coating process. Environmental considerations motivate us to utilize sulfuric acid anodizing to replace chromic acid anodizing. The combination of two coating processes provides composite protection layers including an anodized layer and a nano-particle reinforced layer to aluminum alloy. Electrochemistry tests are conducted to evaluate the properties of galvanic corrosion resistance of aluminum alloy with nano-composite coating. Next, CARALL is fabricated using aluminum alloy sheet with nano-composite coating and commercially available CFRP prepreg. The curing process using an autoclave is the same with that used for the fabrication of conventional carbon fiber/epoxy laminates without aluminum layers. The microstructure of cross-section of CARALL is investigated by means of scanning electron microscope (SEM) and electron probe micro analyzer (EPMA). Corrosion tests of aluminum alloy with and without nano-composite coating are conducted. Furthermore, the internaminar shear strength is evaluated based on three-point and five point bending tests.

## 2 Nano-composite Coating

Commercially available aluminum alloy sheet (2024-T3) of 0.5 mm thickness and Toray T300/#2580 CFRP prepreg of 0.219 mm thickness are used as the metal layer and CFRP layer, respectively. In order to provide a galvanic corrosion protection to aluminum alloy sheet, a new surface treatment method of nano-composite coating is developed. A schematic illustration of nano-composite coating and its application to CARALL is given in Fig. 1. Nano-composite coating consists of two coating layers, namely a sulfuric acid anodized

Al<sub>2</sub>O<sub>3</sub> layer and a SiO<sub>2</sub> nano-particle reinforced inorganic/organic hybrid sol-gel coating layer.

At first, the sulfuric acid anodizing is conducted for 2024-T3 aluminum alloy sheet following a conventional anodizing process. An anodic oxidation coating, namely an Al<sub>2</sub>O<sub>3</sub> layer is formed on the surface of the 2024-T3 sheet and the thickness of the Al<sub>2</sub>O<sub>3</sub> layer is controlled around 3 micrometer. The utilization of sulfuric acid anodizing is based on the consideration of corrosion resistance, material strength, and environmental protection although the sulfuric acid anodizing is not effective as chromic acid anodizing for the corrosion protection of aluminum alloy. It is well known that

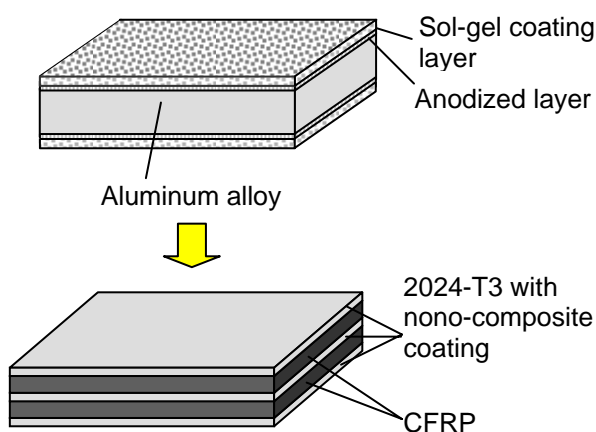


Figure 1. Schematic illustration of nano-composite coating and its application to CARALL

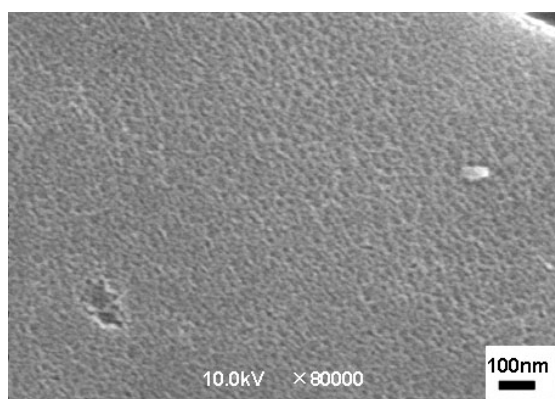


Figure 2. Micro—structure of the anodized surface of aluminum alloy 2024-T3

an anodized film generally contains a very thin lower barrier layer and an upper porous layer. Figure 2 show the SEM image of the porous microstructure of the anodized surface of 2024-T3. Nano-scale porous oxidation layer can be clearly observed. In general, a sealing treatment is carried out by some

hydrothermal processes after anodizing to reduce porosity of the anodic oxidation coating. However, a sealing treatment usually induces weak adhesive properties of the anodic oxidation coating. According to the adhesive and corrosion resistance requirements of CARALL, the present study omits the conventional sealing treatment after the sulfuric acid anodizing. A silica nano-particle reinforced inorganic/organic hybrid sol-gel coating is conducted on the anodized surface of 2024-T3 instead of conventional sealing treatment.

Silica nano-particle reinforced inorganic/organic hybrid sol-gel coating is carried out following the coating method developed by Schmidt et al.<sup>14</sup> Materials used in the hybrid sol-gel coating include 3-glycidyloxypropyltrimethoxysilane (GPTS), bisphenol-A epoxy (EP), colloidal solution of SiO<sub>2</sub> particles (SiO<sub>2</sub>), tetraethylenepentamine (TEPA) as curing agent, ethanol, and distilled water. The diameter of SiO<sub>2</sub> particles in the colloidal solution is around 8-11 nm and the particle content is 20% in weight. It is expected that these SiO<sub>2</sub> nano-particles may reduce the porosity of anodic oxidation coating and improve the mechanical properties of sol-gel coating. Concrete coating process mainly includes three steps, namely a step of the synthesis of sol-gel solution, a dip coating step, and a curing step. Firstly, the pre-hydrolyzation of GPTS is conducted by adding distilled water into GPTS and then stirring the solution for 2 or more hours at room temperature (about 20 degree Celsius). The molar ratio of GPTS to distilled water is about 1:2-3. Then colloidal solution of SiO<sub>2</sub> particles is added into the transparent solution and the solution is stirred continually for about 30 minutes until the solution becomes homogeneously colorless and transparent. The molar ratio of GPTS to SiO<sub>2</sub> is 1:0.7-1.2. Separately, the second solution is prepared by adding EP into ethanol, the molar ratio of GPTS to EP is 1:0.07-0.13, and the molar ratio of GPTS to ethanol is 1:7-10. The solution is stirred for about 1 or more hours at room temperature also until the solution becomes homogeneously colorless and transparent. After the preparation of the two solutions, the second solution with EP is added into the first solution with GPTS. Finally, the synthesis of sol-gel solution is finished by adding the curing agent TEPA into the mixed solution for the organic crosslink reaction and stirring the solution for about 10 minutes. The molar ratio of GPTS to TEPA is 1:0.07-0.12.

After the completion of sol-gel solution preparation, a dip coating process is conducted by

immersing the anodized 2024-T3 aluminum alloy sheet into the solution and then raising it. Afterwards, the aluminum 2024-T3 sheet with dip coated sol-gel solution is immediately cured at 50-130 degree Celsius for 30-90 minutes in an electric oven. In order to obtain fine coating two times of dip coating and curing are conducted. In the first time dip coating, the curing temperature is controlled at 50 degree Celsius for 30-90 minutes. However, in the second time dip coating the curing temperature depends on the applications of the coated 2024-T3 sheet. That is, if the coated 2024-T3 sheet is only used for the electrochemistry tests the curing temperature for the second time coating is controlled at 130 degree Celsius for 90 minutes. On the other hand, if the coated 2024-T3 sheet is used as the metal layer to fabricate CARALL, the curing temperature for the second time coating is controlled at 50 degree Celsius for 30 minutes or the second dip coated 2024-T3 sheet is just put into a desiccator at room temperature for one night according to the consideration of the curing process in the fabrication of CARALL. A SEM image of the cross section of 2024-T3 sheet with nano-composite coating is shown in Fig. 3. We can see that the anodic oxidation coating is about 3 micrometer thick

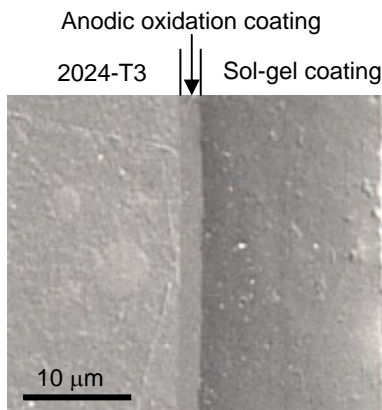


Figure 3. SEM image of cross-section of 2024-T3 sheet with nano-composite coating

and the silica nano-particle reinforced hybrid sol-gel coating is about 15 micrometer thick. Good adhesive situation can be observed along the interface between anodic oxidation coating and sol-gel coating. In order to confirm whether some  $\text{SiO}_2$  nano-particles have been inserted into the pores of anodic oxidation coating, Line analysis of elements is performed using EPMA and the line profiles of various elements are presented in Fig. 4. The area of horizontal axis marked by a dashed ellipse denotes

the interfacial region. We can see that some of  $\text{SiO}_2$  nano-particles have been indeed inserted into the anodic oxidation layer. Hence, this composite coating is expected to provide effective galvanic corrosion protection for 2024-T3.

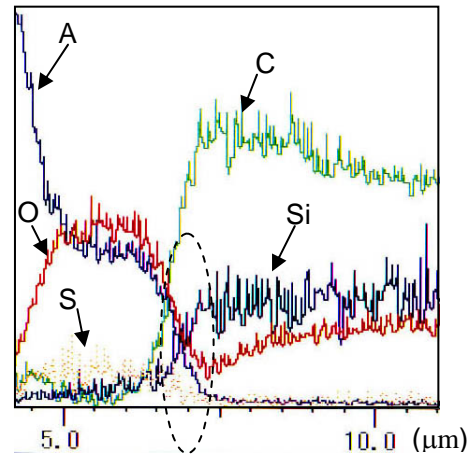


Figure 4. EPMA mapping line profile of cross-section of 2024-T3 sheet with nano-composite coating

### 3 Electrochemistry Tests

In order to investigate the validity of the composite coating for the galvanic corrosion protection of 2024-T3, two kinds of electrochemistry tests, namely natural potential measurement and galvanic corrosion current measurement are performed. The testing area of specimens of 2024-T3 and CFRP is  $100 \text{ mm}^2$ . For a comparison, virgin 2024-T3 specimen (2024-T3), 2024-T3 only with anodizing coating (A-2024-T3), and 2024-T3 only with sol-gel coating (S-2024-T3) are also tested together with 2024-T3 with composite coating (AS-2024-T3) and CFRP. 8 specimens for each case are tested in two kinds of tests. The CFRP specimen is cut from a CFRP laminate of  $[0/90]_{8s}$  fabricated by T300/#2580 prepreg and autoclave curing process. The curing temperature of CFRP laminate is 130 degree Celsius.

The natural potential test is performed using a potentiostat (Hokuto Denko Inc. HA151). A schematic illustration of the natural potential test is shown in Fig. 5. 3% NaCl water is used as test solution, the temperature of the solution is controlled at 35 degree Celsius and the solution is stirred continually by an air pump during the whole test duration. Following the conventional natural potential test, an Ag/AgCl saturated KCl electrode

was used as the reference electrode and a Pt electrode as the counter electrode. The potential difference between the reference electrode and the specimen electrode is measured. The testing duration is one hour.

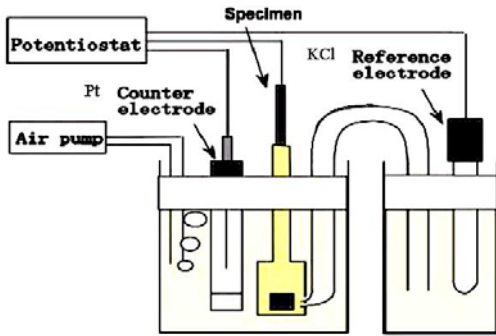


Figure 5. Diagram of natural potential test

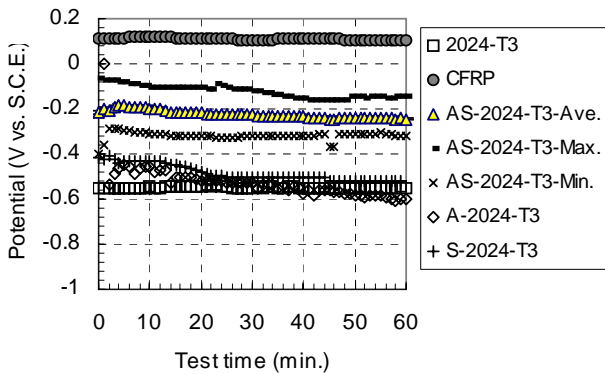


Figure 6. Results of natural potential test

The test results are described in Fig. 6. It is seen that the natural potential of CFRP is about 0.15 V and the potential of the virgin 2024-T3 is about -0.55 V. The potential difference is 0.7 V. A-2024-T3 (2024-T3 with anodizing coating only) and S-2024-T3 (2024-T3 with sol-gel coating only) show the almost same potential with the virgin 2024-T3 although a little higher potential can be observed in the early time. These results reveal the influence of the nano-porous or micro-porous existed in the anodic oxidation film and sol-gel coating on the natural potential. That is, it is not sufficient for the galvanic corrosion protection of 2024-T3 to only use anodizing coating or sol-gel coating. In contrast, AS-2024-T3 (2024-T3 with composite coating) shows a high potential of average -0.2 V which is closed to the natural potential of nickel. Then the potential difference between CFRP and AS-2024-T3 is reduced to 0.35 V that is a half of original potential difference between CFRP and virgin 2024-T3. This

fact proves that the composite coating can greatly improve the corrosion-resistance of 2024-T3 as expected. It is considered that the nano-particles of SiO<sub>2</sub> in the sol-gel coating play an important role in sealing off the nano-scale and micro-scale voids existed in the anodic coating. Consequently, the probability of the solution penetrating the coating layers and reaching the metal surface is rapidly reduced.

In order to confirm the validity of the composite coating for the galvanic corrosion protection of 2024-T3, the galvanic corrosion current is also measured by the use of an electrometer (Takeda Riken TR8651). 3%NaCl water is also used as the test solution. The solution was stirred continually by an air pump during the whole test period and the temperature is controlled at 35 degree Celsius, which is as the same as in the test of natural potential measurement. The schematic illustration of the corrosion current test is described in Fig. 7. The current occurred between CFRP electrode and the specimen electrode due to the natural potential difference of two electrodes is measured. The testing period is one hour. Test results are described in Fig. 8. The corrosion current occurred between CFRP and 2024-T3 shows the value of  $2.0 \times 10^{-5}$  (A) and the corrosion current occurred between CFRP and A-2024-T3 also shows the same value. It is a little different for S-2024-T3 which gives a relatively small corrosion current value close to  $3.0 \times 10^{-6}$  (A). In contrast, AS-2024-T3 (with composite coating) gives a much smaller corrosion current value close to  $3.0 \times 10^{-10}$  (A). The corrosion current of AS-2024-T3 is reduced by about 5 orders compared with virgin 2024-T3. The above facts confirm that the composite coating can indeed provide effective protection for 2024-T3 from galvanic corrosion.

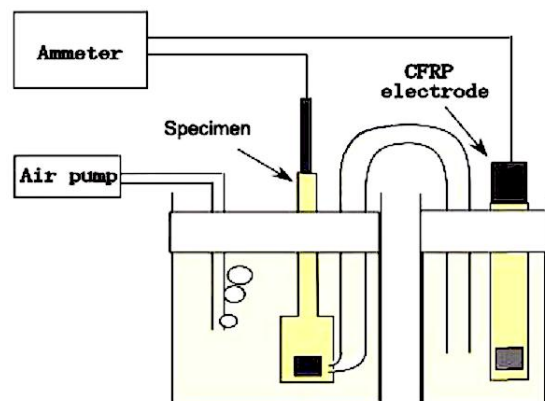


Figure 7. Diagram of corrosion current

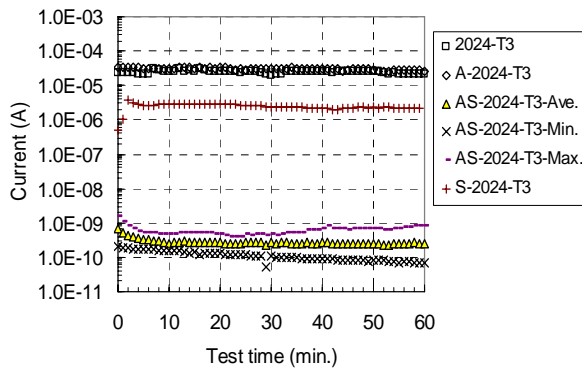


Figure 8. Results of corrosion current test

#### 4 Fabrication of CARALL and Corrosion Test

CARALL is fabricated using unidirectional CFRP prepreg (TORAY T300/#2580) and the 2024-T3 sheet of 0.5 mm thickness with composite coating. The stacking sequence of the laminate is [Al/0/90/90/0/Al]. The stacked CARALL is cured in an autoclave following the curing process provided by TORAY. The curing cycle is as the same as that used in the fabrication of conventional CFRP laminate without aluminum layer. No extra adhesive film need to bind the aluminum sheet with CFRP prepreg. Figure 9 shows the photograph of a

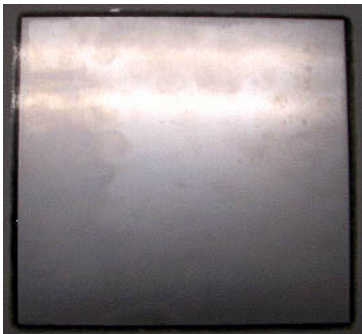


Figure 9. Fabricated CARALL

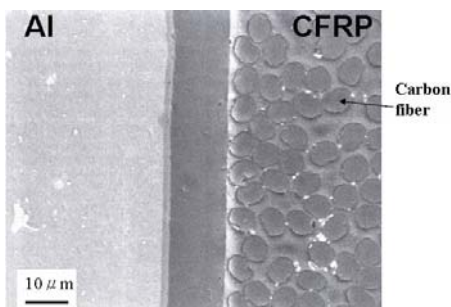


Figure 10. SEM image of CARALL's cross-section

CARALL fabricated at our laboratory. The thickness of the CARALL is about 1.8 mm. The SEM image of the cross section of CARALL is shown in Fig. 10. It is seen that a well bonded composite coating layer has been formed between CFRP and 2024-T3 sheet and that no obvious voids can be observed at present micro-scale. Figure 11 shows the EPMA mapping image of Si to investigate the distribution of SiO<sub>2</sub> nano-particles, and the upper picture is the corresponding SEM image. It is observed that SiO<sub>2</sub> nano-particles seem to be uniformly distributed in the sol-gel coating layer as expected.

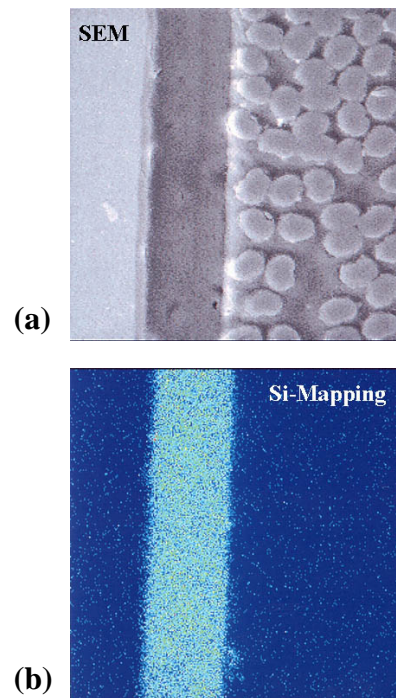


Figure 11. (a) SEM image and, (b) EPMA mapping of Si of cross-section of CARALL

In addition of electrochemistry tests for the individual samples of aluminum alloy and CFRP, corrosion test of CARALL is also performed by immersing the specimens of CARALL into 3% NaCl solution at room temperature for 300 hours and 900s hour to investigate the corrosion resistance of CARALL. The specimen is cut from the CARALL plate as shown in Fig. 9, and the geometry of specimen is of 130 mm length, 13 mm width and 1.5 mm thickness. The side surface is polished by the use of sand paper until #4000 for the sake of surface observation. Two specimens are tested for each case of 300 hours and 900 hours. Virgin 2024-T3 and S-2024-T3 (only sol-gel coating) are also tested for a comparison. Test results are given in Fig. 12 and Fig. 13. The images of corrosion damage on the top

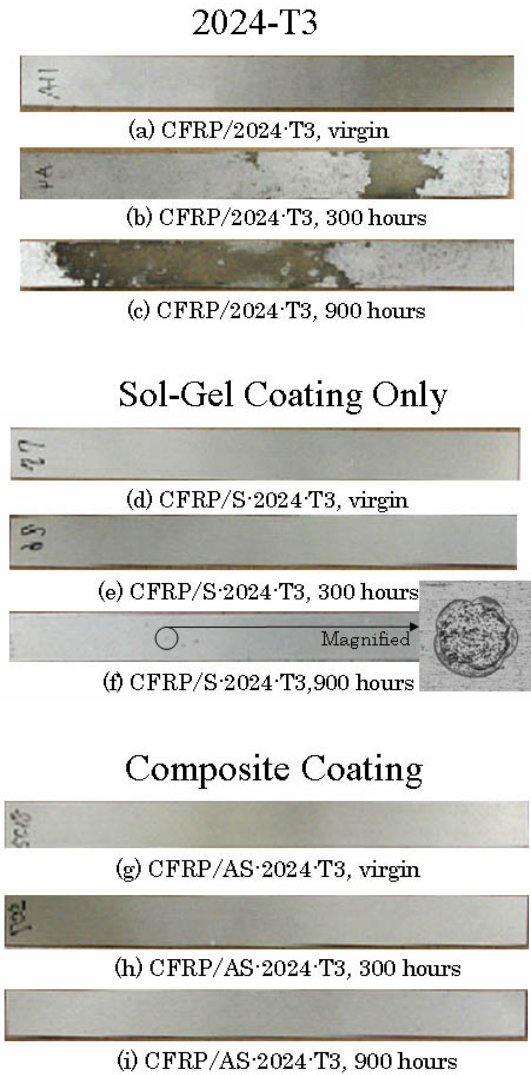


Figure 12. Corrosion damage on the top surface

surface of specimens are shown in Fig. 12. In the case of virgin 2024-T3, severe corrosion can be seen on the surface of CFRP/2024-T3 in the both images of 300 hours and 900 hours. Corrosion damage obviously progresses as the immersing time increases. In the case of CFRP/S-2024-T3, no obvious corrosion can be seen in the image of 300 hours, but some point corrosion can be observed in the image of 900 hours. In contrast, the CFRP/AS-2024-T3 (with composite coating) shows no any corrosion damage on its top surface even after 900 hours immersion. This fact is consistent with the results of electrochemistry tests and proves again that the composite coating provides effective corrosion protection for CARALL. In Fig. 13, the side surface images of CFRP/AS-2024-T3 of virgin and after 900 hours are presented together with

2024-T3 after 900 hours and S-2024-T3 after 900 hours. These images are different from those of Fig. 12 because all the side surfaces are polished by sand paper. Hence, severe corrosion damage can be seen in all kinds of specimens after 900 hours immersion. At present observation, no obvious corrosion difference can be observed from these specimens. However, delamination between CFRP and aluminum sheet was observed only in the case of CFRP/2024-T3. This fact may reflect the influence of galvanic corrosion on the interlaminar strength between CFRP and aluminum sheet.

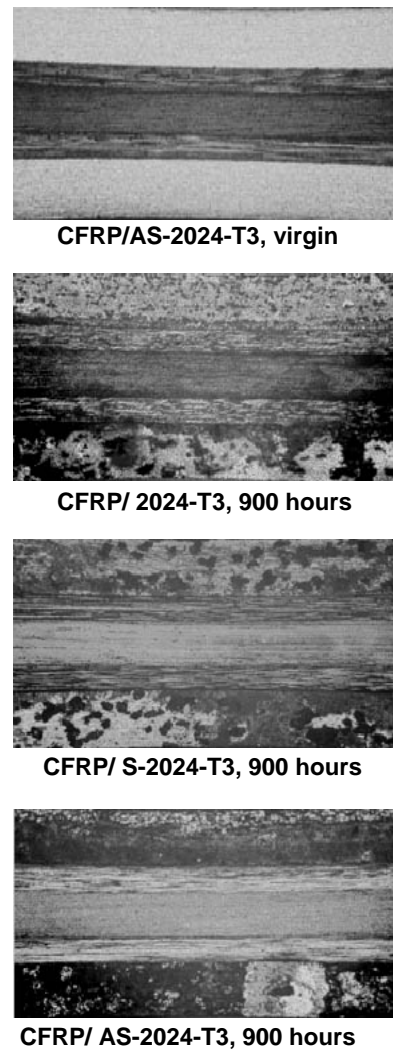


Figure 13. Corrosion damage on the side surface

### 5 Interlaminar Shear Strength

Three-point and five-point bend tests are performed to evaluate the interlaminar shear strength of fabricated CARALL, as shown in Fig. 14. Specimen shown in Fig. 15 is cut from a laminate.

The upper and lower layers of specimen are aluminum alloy 2024-T3 of 0.5 mm thickness and the mid-layer is unidirectional CFRP (T300/#2580) of 8 plies. A nano-composite coating is conducted on the aluminum surface to prevent CARALL from galvanic corrosion before the fabrication of CARALL. The total thickness of laminated beam is about 1.8 mm. Specimen width B is 10 mm, specimen length is 50 mm. The testing length L is 12 mm for three-point bend test and 10 mm for five-point bend test. Seven specimens are tested in three-point bend case and five specimens are tested in five-point bend case. The interlaminar shear strength is evaluated from following equations derived based on classic beam theory [17].

$$ILSS = \tau_{xy}(h_2) = \frac{3P_{max}}{4Bt^*} \quad (\text{three-point bend}) \quad (1)$$

$$ILSS = \tau_{xy}(h_2) = \frac{33P_{max}}{64Bt^*} \quad (\text{five-point bend}) \quad (2)$$

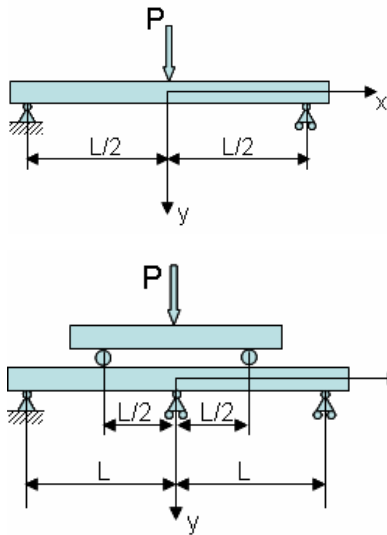


Fig. 14 Three-point and five-point bend tests

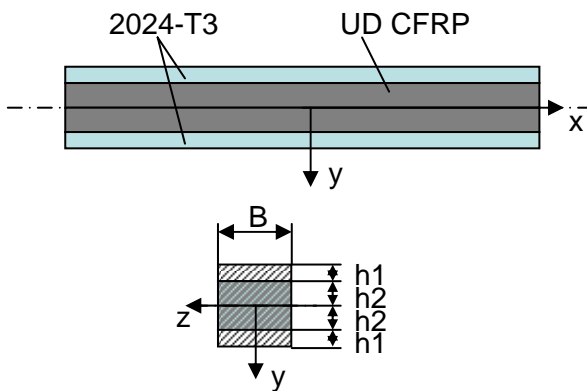


Fig. 15 Configuration of specimen

$$t^* = \frac{2\{E_1[(h_1 + h_2)^3 - h_2^3] + E_2h_2^3\}}{E_1(h_1^2 + 2h_1h_2)} \quad (3)$$

where  $t^*$  represents an effective thickness of specimen,  $E_1$  the Young's modulus of 2024-T3, and  $E_2$  the modulus of fiber direction of unidirectional CFRP.

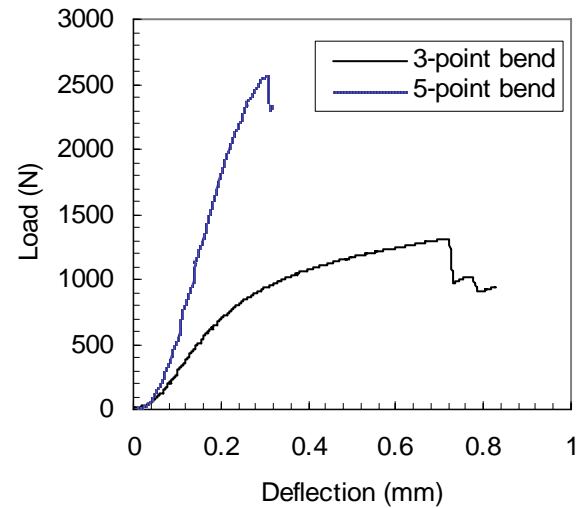


Fig. 16 Typical load-deflection curves

Bend tests are performed using a MTS material testing system. The loading rate is 1.0mm/min. Typical load-deflection curves are presented in Fig. 16. It is seen that three-point bend test gives very different load-deflection curve from five-point bend test. This feature is also can be observed from the test results of interlaminar shear strength, as presented in Table 1 and Table 2. From these tables it is seen that two kinds of bend test give very different values of interlaminar shear strength. The average value of interlaminar shear strength is about 46.12 MPa for three-point bend tests, but 64.26 MPa for five-point tests. Similar results can be found in [8]. Why do two kinds of bend tests lead to so different load-deflection curves and ILSS results? Detail finite element analysis is conducted in [17], which reveals that large deflection in three-point bend test cause large scale plastic deformation along and close to the interface. Consequently, large scale plastic deformation along and close to the interface leads to a low interlaminar shear strength in three-point bend tests. Thus, it is considered that the five-point bend is more suitable for the evaluation of interlaminar shear strength when the interface of specimen is not on the mid-plane. For a reference, the interlaminar shear strength of T300/#2500 is



about 98 MPa from the data of Toray’s homepage. It is considered that the present interlaminar shear strength of CARALL is a reasonable value.

**Table 1 Results of 3-point bend test**

3-point bend		
specimen No.	Pmax N	shear stress MPa
1	1017	39.9290756
2	1246	47.271
3	1196	49.2474878
4	1034	42.0638675
5	1346	51.6451023
6	1363	46.021695
7	1106	46.6801125
Average		46.1226201

**Table 2 Results of 5-point bend test**

3-point bend		
specimen No.	Pmax N	shear stress MPa
1	2472	66.7250288
2	2448	58.8874645
3	2802	62.844393
4	2575	66.0491768
5	2589	66.777214
Average		64.25666

**6 Conclusion**

A new galvanic corrosion-resistant CARALL is developed based on nano-composite coating. The nano-composite coating consists of a sulfuric acid anodizing and a silica nano-particle reinforced hybrid sol-gel coating. Microstructures of nano-composite coating are investigated. Electrochemistry tests and corrosion test by immersing the CARALL specimen into 3%NaCl solution for a long time are conducted and the results prove that the composite coating greatly improve the corrosion-resistance of 2024-T3. Furthermore, CARALL is fabricated following conventional curing process of CFRP without aluminum layers and its interlaminar shear strength is investigated by three-point and five-point bend tests. It is found that three-point bend test gives lower evaluation than five-point bend test because of the large scale plastic deformation and that five-point bend test is more suitable for the experimental evaluation of the interlaminar shear strength of CARALL. In other words, the five point bend test is

more available than three-point bend test for the evaluation of the interlaminar shear strength of a laminate whose interface between layers of dissimilar materials is not on the mid-plane of the laminate.

**Acknowledgments**

This work was supported by the Ministry of Education, Culture, Sports, Science and Technology of Japan under a grant-in-aid (No. 16560600) for Science Research.

**References**

- [1] Asundi, A., and Choi, A. Y. N., “Fiber Metal Laminates: An Advanced Material for Future Aircraft,” *Journal of Materials Processing Technology*, Vol. 63, 1997, pp. 384-394.
- [2] Vogelesang, L. B., and Vlot, A., “Development of Fiber Metal Laminates for Advanced Aerospace Structures,” *Journal of Materials Processing Technology*, Vol. 103, 2000, pp. 1-5.
- [3] Vlot, A., and Gunnink, J. W., *Fiber Metal Laminates: An Introduction*, Kluwer Academic Publishers.L.B. 2001, pp. 14-21.
- [4] Lin, C. T., Kao, P. W., and Yang, F. S., “Fatigue Behavior of Carbon Fiber-Reinforced Aluminum Laminates,” *Composites*, Vol. 22, No. 2, 1991, pp. 135-141.
- [5] Vermeeren, C. A. J. R., “The application of carbon fiber in ARALL Laminates”, Delft University of Technology, Report LR-658, 1991.
- [6] Lin, C. T., Kao, P. W., and Jen, M. -H. R., “Thermal Residual Strains in Carbon Fiber-Reinforced Aluminum Laminates,” *Composites*, Vol. 25, No. 4, 1994, pp. 303-307.
- [7] Afaghi-Khatibi, A., Ye, L., and Mai, Y. W., “Evaluations of Effective Crack Growth and Residual Strength of Fiber-Reinforced Metal Laminates with a Sharp Notch,” *Composites Science and Technology*, Vol. 56, 1996, pp. 1079-1088.
- [8] Lawcock, G., Ye, L., Mai, Y. W., and Sun, C. T., “The Effect of Adhesive Bonding Between Aluminum and Composite Prepreg on the Mechanical Response of Carbon-Fiber-Reinforced Metal Laminates,” *Composites Science and Technology*, Vol. 57, 1997, pp. 35-45.
- [9] Lawcock, G., Ye, L., Mai, Y. W., and Sun, C. T., “Effects of Fiber/Matrix Adhesion on Carbon-Fiber-Reinforced Metal Laminates-I. Residual Strength,” *Composites Science and Technology*, Vol.57, 1997, pp.1609-1619.
- [10] Lawcock, G., Ye, L., Mai, Y. W., and Sun, C. T., “Effects of Fiber/Matrix Adhesion on Carbon-Fiber-Reinforced Metal Laminates-II. Impact

- Behavior,” *Composites Science and Technology*, Vol.57, 1997, pp.1621-1628.
- [11] Ye, L., Afaghi-Khatibi, A., Lawcock, G. D., and Mai, Y. M., “Effect of Fiber Adhesion on Residual Strength of Notched Composite Laminates,” *Composites Part A*, Vol.29A, 1998, pp.1525-1533.
- [12] Afaghi-Khatibi, A., Lawcock, G. D., Ye, L., and Mai, Y. M., “On the Fracture Mechanical Behavior of Fiber Reinforced Metal Laminates (FRMLs),” *Comput. Methods Appl. Mech. Engrg.*, Vol. 185, 2000, pp. 173-190.
- [13] Twite, R. L., and Bierwagen, G. P., “Review of Alternatives to Chromate for Corrosion Protection of Aluminum Aerospace Alloys,” *Progress in Organic Coatings*, Vol. 33, 1998, pp. 91-100.
- [14] Schmidt, H., Langenfeld, A., and Naß, R., “A New Corrosion Protection Coating System for Pressure-Cast Aluminum Automotive Parts,” *Materials & Design*, Vol. 18, 1997, pp. 309-313.
- [15] Conde, A., Durán, A., and de Damborenea, J. J., “Polymeric Sol-Gel Coatings as Protective Layers of Aluminum Alloys,” *Progress in Organic Coatings*, Vol. 46, 2003, pp. 288-296.
- [16] Du, Y. J., Damron, M., Tang, G., Zheng, H., Chu, C. J., Osborne, J. H., “Inorganic/Organic Hybrid Coatings for Aircafte Aluminum Alloy Substrates,” *Progress in Organic Coatings*, Vol. 41, 2001, pp. 226-232.
- [17] Wang, W. X., Higashijima, M., Takao, Y., and Matsubara, T. “Test methods for evaluating the interlaminar shear strength of CFML,” Proceedings of International Conference on Advanced Technology in Experimental Mechanics 2007, Paper No. ATEM07-90286, Fukuoka, Japan, 2007.